JOURNAL OF GEOPHYSICAL RESEARCH, VOL. 103, NO. B4, PAGES 7363–7370, APRIL 10, 1998

Geothermics and climate change
1. Analysis of borehole temperatures with emphasis on resolving power

Robert N. Harris

Rosenstiel School of Marine and Atmospheric Science, University of Miami, Miami, Florida

David S. Chapman

Department of Geology and Geophysics, University of Utah, Salt Lake City.

Abstract. Temperature-depth data from six boreholes in western Utah and nine boreholes in southeastern Utah are reanalyzed for evidence of ground surface temperature (GST) histories. We invert the temperature-depth data using the functional space inverse algorithm of *Shen and Beck* [1991, 1992] which we prefer over previous inversions of these data because of its greater sophistication and flexibility in suppressing noise. GST histories for western and southeastern Utah are generally consistent and suggest that temperatures in the mid-1800s are, on average, cooler than previous centuries, followed by about 0.6°C of warming in this century. Attention is given to the temporal resolution of our GST solutions showing the time-smearing effects of heat conduction on the solutions. GST solutions represent an average ground temperature over a time window that expands as we look farther into the past. The size of the time window is a function of measurement and geologic noise and limits the ultimate resolution of GST reconstructions.

1. Introduction

Over the past decade, there has been growing concern that increases in the concentration of greenhouse gases in Earth's atmosphere are linked to surface warming. Perhaps the most intuitive and best studied signals of warming are surface air temperature (SAT) time series. Globally averaged SATs indicate relatively constant temperatures between 1860 and 1890, warming to 1950, a weak cooling trend to 1960, and a strong warming trend to the present. Overall, the SATs indicate an average warming of 0.45° ± 0.15°C over the past 100 years [*Folland et al.*, 1990]. The SAT record, however, suffers from data inhomogeneities caused by changes in the time of observation, changes in instrumentation, station relocations, and missing data, all of which contaminate raw SAT time series [*Karl and Quayle*, 1988]. While adjustments for these inhomogeneities have been applied to SAT data [*Karl et al.*, 1986; *Karl and Williams*, 1987], it has been difficult to find independent data to test these adjustments. To compound the problem of assessing trends in SAT data that may be related to industrialization, most SAT time series do not extend to times prior to the twentieth century.

An independent source of information about the Earth's changing surface temperature is contained in borehole temperature-depth measurements. In the absence of moving fluids, changes in ground surface temperatures (GST) diffuse slowly downward through rock by the process of heat conduction and are manifested at a later time as anomalies to Earth's background temperature profile. These temperature anomalies are a direct thermophysical outcome of changing ground surface temperatures, not a proxy for it. Once temperature-depth data have been rigorously screened to ensure that the anomalous temperatures are not explained in terms of nonclimatic processes, they may be interpreted in terms of a GST history [*Lachenbruch and Marshall*, 1986] (see also review by *Lewis* [1992]). Depth and time are linked nonlinearly by thermal diffusivity; temperature changes that occurred 100 years ago have penetrated to only 80 m, whereas changes that occurred 1000 years ago have penetrated to 300 m. Boreholes of several hundred meters depth therefore potentially contain a response of the solid Earth to ground temperature histories over the last millennium and are therefore particularly well-suited to extend estimates of surface temperature histories to preindustrial times. Heat conduction unfortunately also smears the climate signal. Thus high-frequency components are diffused out with time, leaving a temporally "smeared" but robust and direct signal of long-wavelength temperature variations at the Earth's surface.

While the recovery of past GST histories from borehole temperature-depth measurements has been known for some time [e.g., *Lane*, 1923; *Birch*, 1948], *Lachenbruch and Marshall* [1986] first pointed out that the magnitude and timing of ground surface warming in the Alaskan Arctic is consistent with models of greenhouse warming. Ensuing results from North America [*Deming*, 1995] indicate 1°-2°C of warming in central and eastern Canada [*Beltrami and Mareschal*, 1991, 1992; *Wang and Lewis*, 1992; *Wang et al.*, 1994], warming between 0° and 2°C for the northern U. S. plains [*Gosnold et al.*, 1997], 1.2°-1.5°C of warming in north central Oklahoma [*Deming and Borel*, 1995], an average of 0.6°C warming in the northern Basin and Range of Utah [*Chisholm and Chapman*,

Paper number 97JB03297.
0148-0227/98/97JB-03297$09.00

1992; *Chapman et al.*, 1992], and between 0.5° and 0.8°C warming in southeastern Utah [*Harris and Chapman*, 1995]. Although the timing of warming is not well constrained, these studies indicate that ground warming has occurred over the past 100 to 200 years. As a whole, these results show an increase in the magnitude of warming with increasing latitude consistent with the latitudinal variation observed in SAT records [*Hansen and Lebedeff*, 1987] and general circulation models [*Wigley and Barnett*, 1990].

The primary purpose of this study is to document the benefits of analyzing borehole temperature profiles in combination with SAT records. These benefits include (1) an ability to enhance the confidence that both records are responding to similar changes in surface temperatures and (2) the establishment of baseline reference temperatures which provide a longer term perspective on contemporary warming reflected in SATs. In this paper, the first of two, we set the stage by describing the record of changing ground surface temperatures manifested in borehole temperature-depth measurements. In a companion paper [*Harris and Chapman*, this issue], we describe a quantitative method for comparing transient borehole signals with SAT records.

Utah provides an ideal opportunity for this type of analysis because many weather stations and boreholes suitable for this complementary analysis are available. Borehole temperature data used in this study have been previously evaluated but with two different inverse techniques. The data from western Utah [*Chisholm and Chapman*, 1992] have been interpreted in terms of ramp functions, while the data from southeastern Utah [*Harris and Chapman*, 1995] have been interpreted using a singular value decomposition (SVD) algorithm with solutions parameterized in terms of a series of step functions. However, because the boreholes in southeastern Utah penetrate sedimentary strata, an inherently noisy environment to reconstruct GST histories, relatively few eigenvectors were used, and the solutions were well approximated by ramp functions. In both studies, coherent trends remained in the temperature-depth data that could not be fit by these simple parameterizations. We now believe that the functional space inversion (FSI) of *Shen and Beck* [1991, 1992] can provide superior resolution, especially in the recent past, relative to ramp or staircase solutions without unduly increasing solution variance. *Shen et al.* [1996] pointed out that in the presence of noise FSI gives superior results to SVD, particularly when the mean of the transient differs from the steady state temperature field. We feel that the FSI approach has the potential to capture GST signals with higher fidelity than these previous studies and thus makes it ideal for comparing borehole transients with SAT time series from the same area.

2. Borehole Temperatures and Functional Space Inversion

Borehole temperature profiles are analyzed using the FSI algorithm of *Shen and Beck* [1991, 1992] a nonlinear least squares inversion based on the theory of *Tarantola and Valette* [1982a, b] and *Tarantola* [1987]. This algorithm is based on one-dimensional heat conduction in a layered half-space with a temperature-depth distribution assumed to be composed of two components (1) a steady state component governed by the long-term mean surface ground temperature, heat flow at the base of the half-space, and variable thermophysical properties of the rocks in which the temperature measurements are made and (2) a transient component assumed to be caused by time variations of the ground surface temperature. An advantage of this approach is the ability to incorporate thermophysical properties and their uncertainties explicitly as model parameters.

The FSI algorithm determines a model that minimizes the misfit function [*Shen et al.*, 1995],

$$S(m)=\frac{1}{2}\left[(d-d_o)^t C_d^{-1}(d-d_o)\right]+\frac{1}{2}\left[(m-m_o)^t C_m^{-1}(m-m_o)\right], \quad (1)$$

where d and d_o are the calculated and observed borehole temperatures, respectively, m is the calculated model, and m_o is the a priori model in which thermophysical rock properties are incorporated. C_d is the covariance matrix of d_o indicating the uncertainty in the observed temperature-depth data. C_m is the covariance matrix of m_o representing uncertainties in the a priori model. The trade-off between the relative sizes of C_d and C_m uniquely determine and stabilize the solution. A small size for C_m weights (1) such that the second term dominates $S(m)$ and corresponds to having great confidence in the a priori model. As the model covariance matrix is increased in size, the weight of C_m on the solution decreases, corresponding to having relatively less confidence in the a priori model, and the solution becomes better resolved by the data. *Shen et al.* [1995] found that the weighting and therefore trade-off in $S(m)$ depends most strongly on the sizes of the a priori standard deviation of the temperature data (σ_{do}) and thermal conductivity (σ_{ko}). If the a priori model is overly constrained (small value of σ_{ko} relative to σ_{do}) then representational errors could corrupt the solution, and boreholes in geographic proximity to each other could yield very different results. In this context, representational errors stem from modeling the real three-dimensional Earth in terms of one-dimensional heat conduction, and, as pointed out in their study, all approaches to date for reconstructing GST histories from borehole temperature-depth measurements are idealized in terms of one-dimensional heat conduction. Their numerical experiments showed that as the inversion is loosened (larger values of C_m relative to C_d) representational errors (subsurface thermophysical heterogeneities) can be suppressed without overly attenuating the GST history signal and that the most effective method is to increase the size of σ_{ko}.

3. Geothermal Data

Borehole temperature logs used in this study consist of high-quality measurements at six sites in western Utah and nine sites in the Colorado Plateau of southeastern Utah, United States (Figure 1). These data come from larger data sets and have already been screened for studies of GST histories [*Chisholm and Chapman*, 1992; *Harris and Chapman*, 1995]. The borehole sites in western Utah penetrate low-permeability, relatively homogenous granites, while those in southeastern Utah penetrate sedimentary sequences. The boreholes in western Utah were drilled to a depth of 150 m (a minimum for climatic change studies) measured in 1978; those in southeastern Utah extend to depths between 300 and 600 m and were measured in late 1979 and early 1980 with the exception of SRD-2 which was measured in 1976. Temperature-depth measurements were made using a thermistor probe, four-conductor cable and a digital resistance meter in stop-go mode.

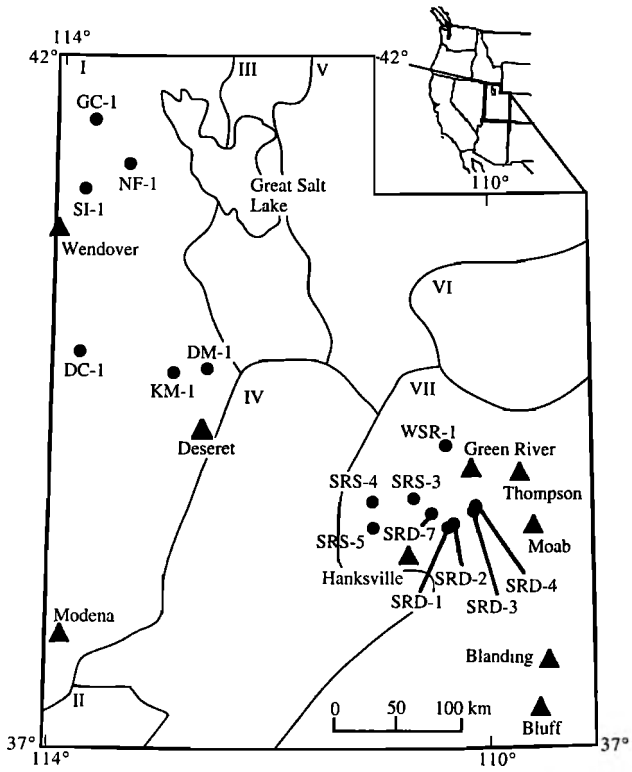

Figure 1. Location map showing boreholes (circles) and meteorological stations (triangles). Bold curves show climatic divisions in Utah which follow drainage divides and are thought to represent areas of relative climatic homogeneity.

All thermistors were calibrated in the laboratory against a Hewlett Packard 2804A quartz thermometer. The precision and accuracy of the measurements are estimated to better than 0.01 K and 0.1 K, respectively [*Bodell and Chapman*, 1982]. Details of instrumentation and measurement procedure are reported by *Chapman* [1976] and *Chapman et al.* [1981]. Nonclimatic sources of disturbances to the background temperature field have been quantitatively considered. Temperature-depth records from these boreholes show no signs of groundwater flow and have only negligible perturbations to the steady state thermal field caused by terrain or vegetation effects (for a complete review see appendix in Chisholm *and Chapman* [1992] and discussion by *Harris and Chapman* [1995]).

Raw temperature-depth profiles are shown in Figures 2a and 3a for western and southeastern Utah, respectively. The temperature profiles are plotted against relative temperature to avoid overlap. Logging starts at a depth of 20 m to avoid the annual temperature cycle. The first-order effect exhibited in these profiles is a general increase of temperature with depth consistent with an upward flux of heat to the Earth's surface. The profiles in western Utah appear to be linear in the deepest part of each borehole. Temperature profiles in southeastern Utah are generally linear within formations; changes in trend between formations are attributable to measured changes in thermal conductivity.

For conductive heat transfer (and assuming constant heat flow), the background temperature field is inversely proportional to thermal conductivity, and thus thermal conductivity variations at each site must be explicitly considered. In both western and southeastern Utah, thermal conductivities were determined using a divided bar apparatus and the cell method described by *Sass et al.* [1971] and calibration procedures given by *Chapman* [1976]. Reproducibility is about 3%; accuracy is based on calibration standards and is estimated to be better than 10%. In western Utah, thermal conductivities for each borehole were determined from drill cuttings, and samples were measured approximately every 16 m. Because thermal conductivity values exhibited only small variations about the mean and most importantly showed no systematic variation as a function of depth [*Chisholm and Chapman*, 1992, Figure A1], a priori thermal conductivities were assigned their mean value (Table 1). In southeastern Utah, thermal conductivity values were determined from solid rock discs for each formation that the boreholes penetrated. *Harris and Chapman* [1995] assuming a constant basal heat flow condition used slightly adjusted values of thermal conductivity (in most cases within 4% of the mean and not exceeding 8% of the mean). A priori thermal conductivities were assigned on a formation by formation basis (Table 2). A priori values of heat capacity were assigned according to the relation $\rho c = k/\alpha$, where ρc is heat capacity (product of density ρ and specific heat c), k is thermal conductivity, and α is thermal diffusivity, assumed to be 10^{-6} m^2 s^{-1}.

4. Inversion Results

As discussed in section 2, the selection of appropriate values of a priori standard deviations for thermal conductivity σ_{ko} and the data σ_{do} is critical to determining GST solutions using the FSI algorithm. Amplitudes of GST histories change as a function of the estimated a priori standard deviations. Warming or cooling signals can be amplified or attenuated through the choice of a priori parameter values, but a warming trend cannot be transformed to a cooling trend or vice versa. Our strategy for finding optimal a priori parameter values of σ_{ko} and σ_{do} follows that of *Shen et al.* [1995]. They assume that boreholes in geographic proximity should give consistent values and that consistency should be achieved without overly attenuating the signals. Accordingly, we solve the inverse problem for a family of parameter values (10 mK $\leq \sigma_{do} \leq$ 400 mK and 0.1 W m^{-1}K^{-1} $\leq \sigma_{ko} \leq$ 4.0 W m^{-1}K^{-1}) and seek the set possessing a satisfactory trade-off between solution consistency and resolution. Our results indicate only slight sensitivity to σ_{do}; however, as the value of σ_{ko} increases, solutions become more consistent but also attenuate. At some point of increasing σ_{ko}, the solutions only slowly increase their consistency but continue to attenuate rapidly. We choose a priori parameter values where solution consistency had for the most part been achieved but before undue attenuation. An adequate trade-off between solution consistency and solution resolution is achieved if a priori standard deviation values of σ_{ko} = 1.0 W m^{-1}K^{-1} and σ_{do} = 50 mK are used for western Utah and σ_{ko} = 2.0 Wm^{-1}K^{-1} and σ_{do} = 50 mK are used for southeastern Utah. The larger σ_{ko} value for southeastern Utah is necessary to attenuate the effects of increased variability of the thermal conductivities (and other thermophysical rock properties) associated with the layered sedimentary environment in which the data were collected. Note that the standard deviations associated with the thermal conductivity measurements in southeastern Utah (Tables 1 and 2) are, on average, twice those of western Utah.

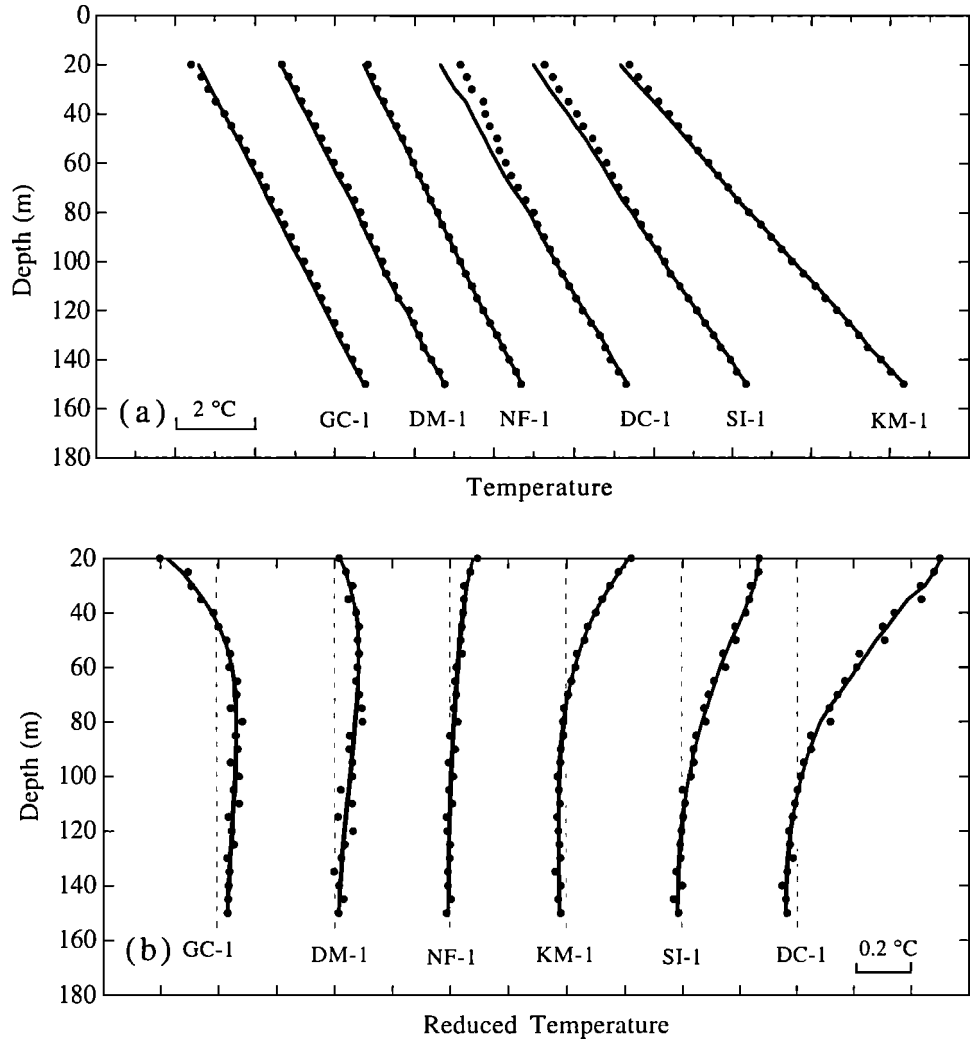

Figure 2. Borehole temperature-depth data for western Utah. (a) Raw temperature-depth data. Circles show individual temperature measurements; solid curves show background temperature field. Temperatures are offset to avoid overlap. (b) Reduced temperatures. Circles show reduced temperature obtained by subtracting background thermal field from raw temperature-depth measurements. Solid curves show transient temperatures ascribed to a changing ground surface condition. The background temperature field and transient temperatures are given by the functional space inversion and together yield the model fit to the data. Relative temperatures are used to avoid overlap.

Preferred solutions for the boreholes in western Utah and southeastern Utah are shown in Figures 2 and 3. Figures 2a and 3a show the raw data with the background thermal regime estimated in the inversion. Kinks in the background thermal regime are the result of a posteriori variations in thermal conductivity. Figures 2b and 3b show reduced temperatures (observed data minus background temperature field) with an expanded temperature scale that illustrates small departures from the background thermal field. High-frequency variations in plotted temperatures indicate the noise level in the data. At four of the six sites in western Utah (Figure 2b), reduced temperatures near the surface are consistently positive, having amplitudes 0.1° to 0.5°C, and extend to depths between 80 and 100 m. Borehole GC-1 has a clear negative reduced temperature anomaly with a maximum amplitude of -0.3°C at 20 m in depth. Borehole DM-1 has only modest positive reduced temperatures between 90 and 45 m that diminish up to 20 m in depth. This borehole is almost twice as noisy as the other boreholes in western Utah. In southeastern Utah (Figure 3b), reduced temperatures near the surface are consistently positive, with amplitudes between 0.2° and 0.5°C and depth extents between 100 and 200 m. Borehole SRS-5, however, shows a negative departure that is greatest at a depth of 70 m. A comparison of these plots shows that the data in southeastern Utah are noisier than the data in western Utah. With the exception of GC-1 in western Utah and SRS-5 in southeastern Utah, these positive reduced temperature profiles are consistent with recent warming. Transient model fits to the data are plotted and show the degree to which we are honoring the data. These models successfully fit the long-wavelength trends without overly emphasizing higher frequencies which we are interpreting as noise. Individual model fits to the data for both western and southeastern Utah account for > 90% of the data variance. The average rms misfit between the reduced temperatures and the best fitting model is 10.9 and 11.5 mK for western and southeastern Utah, respectively. This represents a

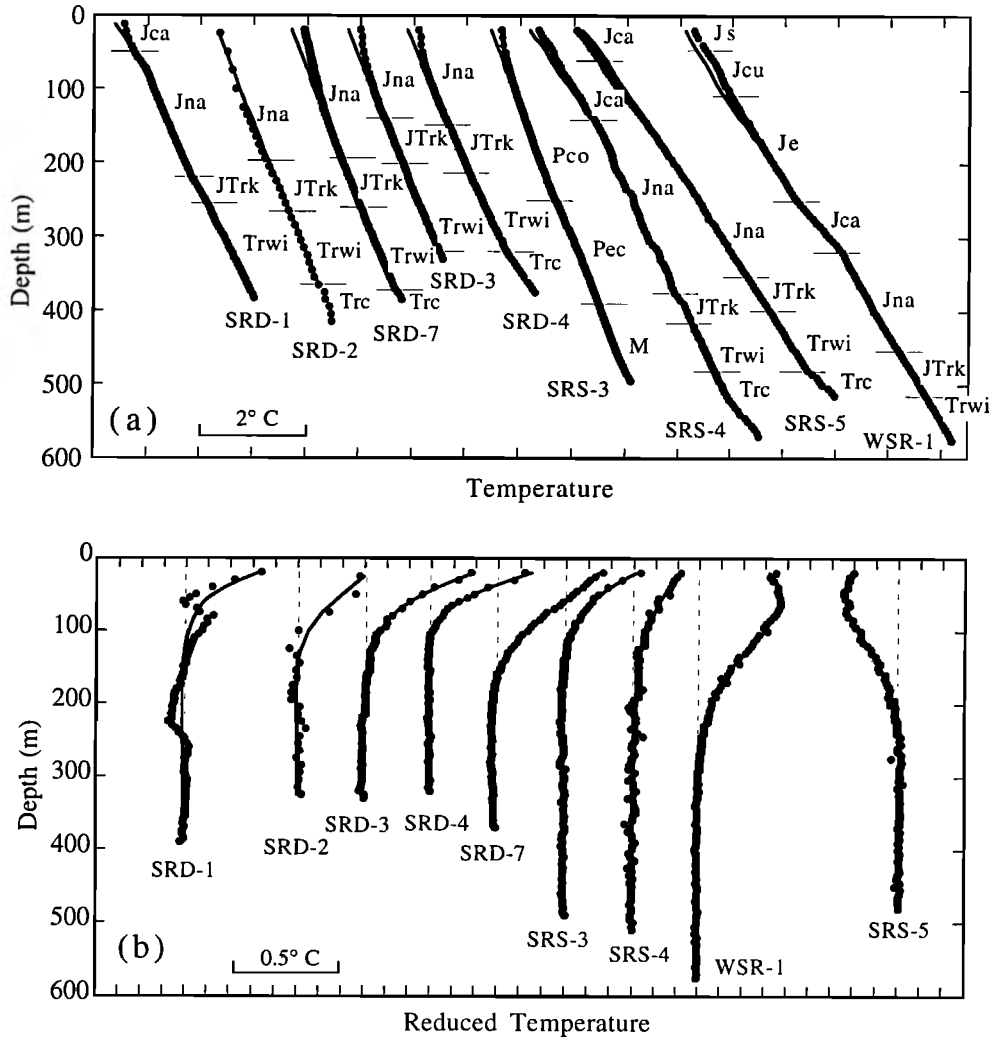

Figure 3. Borehole temperature-depth data for southeastern Utah. (a) Raw temperature-depth data. Circles show individual temperature measurements; solid curves show background temperature field. Temperatures are offset to avoid overlap. (b) Reduced temperatures. Circles show reduced temperatures obtained by subtracting background thermal field from raw temperature-depth measurements. Solid curves show transient temperatures ascribed to a changing ground surface condition. The background temperature field and transient temperatures are given by the functional space inversion and together yield the model fit to the data. Relative temperatures are used to avoid overlap.

significantly better fit to the data than either ramp or step inversions [*Chisholm and Chapman*, 1992; *Harris and Chapman*, 1995] previously employed.

5. Resolution of GST Histories

A fundamental question regarding the use of borehole temperatures to reconstruct GST histories is the resolution. In FSI theory, as well as the theory of *Backus and Gilbert* [1968, 1970], the resolving power is given by the resolution operator (matrix) $\mathbf{R}_m$. In the linear problem

$$\mathbf{d} = \mathbf{G}\,\mathbf{m}. \tag{2}$$

The theory of Backus and Gilbert gives the inverse solution for (2) as

$$\mathbf{m}_{est} = \mathbf{G}^{-g}\,\mathbf{d}_o, \tag{3}$$

where $\mathbf{m}_{est}$ is the a posteriori or the estimated model, $\mathbf{G}^{-g}$ is the generalized inverse, and $\mathbf{d}_o$ is the data vector. The resolution operator is

$$\mathbf{R}_m = \mathbf{G}^{-g}\,\mathbf{G}. \tag{4}$$

In the case of noise free data

$$\mathbf{m}_{est} = \mathbf{G}^{-g}\,\mathbf{d}_o = \mathbf{G}^{-g}\,\mathbf{G}\mathbf{m}_{true} = \mathbf{R}_m\,\mathbf{m}_{true}, \tag{5}$$

where $\mathbf{m}_{true}$ is the unknown but true model. Equation (5) demonstrates that the estimated model $\mathbf{m}_{est}$ is a filtered version of the true model $\mathbf{m}_{true}$, and the filter is the resolution operator $\mathbf{R}_m$. In FSI theory, the incorporation of a priori information gives the inverse solution corresponding to (5) as [*Tarantola*, 1987]

Table 1. A Priori Thermal Conductivities for Western Utah

Site	N	$\bar{k}$ (s.d.), W m^{-1}K^{-1}
GC-1	10	3.14 (0.12)
DM-1	10	3.02 (0.22)
NF-1	17	2.32 (0.17)
DC-1	8	2.55 (0.38)
SI-1	10	2.29 (0.19)
KM-1	10	2.45 (0.14)

N is the number of thermal conductivity samples; $\bar{k}$ is the mean thermal conductivity [*Chisholm and Chapman*, 1992].

$$\mathbf{m}_{est} = \mathbf{G}^{-g}\,\mathbf{d}_o + (\mathbf{I} - \mathbf{R}_m)\,\mathbf{m}_o, \tag{6}$$

where $\mathbf{m}_o$ is the a priori model and $\mathbf{G}^{-g}$ is the generalized inverse in the context of FSI theory. The expression corresponding to (5) is then

$$\mathbf{m}_{est} = \mathbf{R}_m\,\mathbf{m}_{true} + (\mathbf{I} - \mathbf{R}_m)\mathbf{m}_o \tag{7a}$$

or

$$\mathbf{m}_{est} - \mathbf{m}_o = \mathbf{R}_m\,(\mathbf{m}_{true} - \mathbf{m}_o). \tag{7b}$$

With the incorporation of a priori information, it is the deviation of the true model from the a priori model that is being filtered by the resolution operator. Equation (7) shows that the estimated GST history is a weighted average of not only the true and the a priori GST histories but also the true and the a priori values of the other model parameters. Nevertheless, to the extent that the model parameters are tightly constrained and because the a priori GST history is set identically to zero, (7) written for just the GST history will take essentially the same form as (5). Equation (7) has been derived for a linear problem but the concept applies to mildly nonlinear problems as well.

Because the FSI algorithm is only mildly nonlinear, we can use the resolution results of *Clow* [1992]. Using Backus-Gilbert inversion theory, Clow investigated the extent of temporal smearing in GST histories as a function of the maximum error in temperature willing to be tolerated. Clow found that the temporal resolving power or spread $S(\tau_o)$, defined as the finest detail that can be resolved at some time in the past, is proportional to time in the past τ_o and is a function of the ratio of the noise in the data to the noise willing to be accepted in the solution and to the depth of the borehole. With this definition of spread, climatic events occurring in the vicinity of τ_o with duration less than $S(\tau_o)$ cannot be resolved by the available data [*Clow*, 1992]. Use of the a priori estimates of standard deviation with the relation [*Shen et al.*, 1995]

$$\delta d = \frac{q_b}{\lambda}\,\delta z\,\frac{\sigma_{ko}}{\lambda}, \tag{8}$$

where δd is the a priori error and δz is the measurement spacing, permits our results to be cast in terms of those given by *Clow* [1992]. For example, the a priori standard deviations used in western Utah, $\sigma_{do} = 50$ mK and $\sigma_{ko} = 1.0$ W m^{-1}K^{-1}, indicate a total a priori uncertainty of approximately 0.1°C, since the errors propagate as the square-root of the sum of the squares. If we want to limit the error in the GST reconstruction to 0.1°C, then the fractional spread $S(\tau_o)/\tau_o$ is about 1.5 [*Clow*, 1992; Figure 1]. The temperature-depth signal is averaged over a window that is centered at the time in question and has a length of $1.5\tau_o$. If we want to limit the error in our GST solution to ± 0.1°C, our solution will not resolve climatic events shorter than this spread. Of course, by accepting larger error limits, the fractional spread decreases. For southeastern Utah, the fractional spread is approximately $2\tau_o$. The proportionality for each spread is quite large relative to an annual timescale. In summary, because the Earth is a frequency dependent low pass filter, and because of the trade-off between solution spread and variance, average temperatures can be estimated with small errors but at the expense of temporal resolution or spread, When interpreting GST histories, it is important to keep in mind how the loss of temporal resolution increases as we look farther back in time.

GST histories for western and southeastern Utah are shown in Figures 4a and 4b, respectively. Individual GST histories for each borehole are shown as insets. While the plots of transient temperatures (Figures 2b and 3b) apparently show a great deal of variation, it is important to note that the curvature of these temperature depth profiles is mapped into the GST history. Thus while borehole GC-1 has negative anomalous temperatures (Figure 2b), the corresponding early GST history is not radically dissimilar from the other GST histories in western Utah (Figure 4a, inset). Indeed, individual GST histories in western Utah are generally quite consistent. Because the sedimentary strata of southeastern Utah is an inherently more noisy environment, it is not possible to maintain as robust a spread with low solution variance. With the exception of boreholes SRS-5 and WSR-1 (dashed curves Figure 4b, inset), the GST histories in southeastern Utah show modest correlation. Boreholes SRS-5 and WSR-1 were used in the analysis of *Harris and Chapman* [1995] but are now thought not to reflect regional GST histories.

Table 2. Formations and A Priori Thermal Conductivities for Southeastern Utah

Period	Formation	Symbol	Lithology	N	SRD k_a, W m^{-1} K^{-1}	SRS k_a, W m^{-1} K^{-1}	s.d., W m^{-1} K^{-1}
Juarassic	Carmel	Jca	Mdst-Ss	17	---	2.91	0.58
	Navajo	Jna	silty Ss-Ss	24	4.09	4.18	0.72
Triassic	Kayenta	JTrk	silty Ss-Ss	14	3.96	3.86	0.54
	Wingate	Trwi	Ss	17	3.86	4.17	0.37
Permian	Coconino	Pco	Ss	5	---	5.01	0.36
	Elephant Canyon	Pec	Dol-Ss	7	---	4.35	0.63
Mississippian	Redwall	Mr	Dol	2	---	4.82	0.18

N is number of samples; k_a is adjusted thermal conductivity for San Rafael Desert (SRD) and San Rafael Swell (SRS). Lithologies are Ss, sandstone; Mdst, mudstone, and Dol, dolomite. Dashes indicate that boreholes did not intersect these formations.

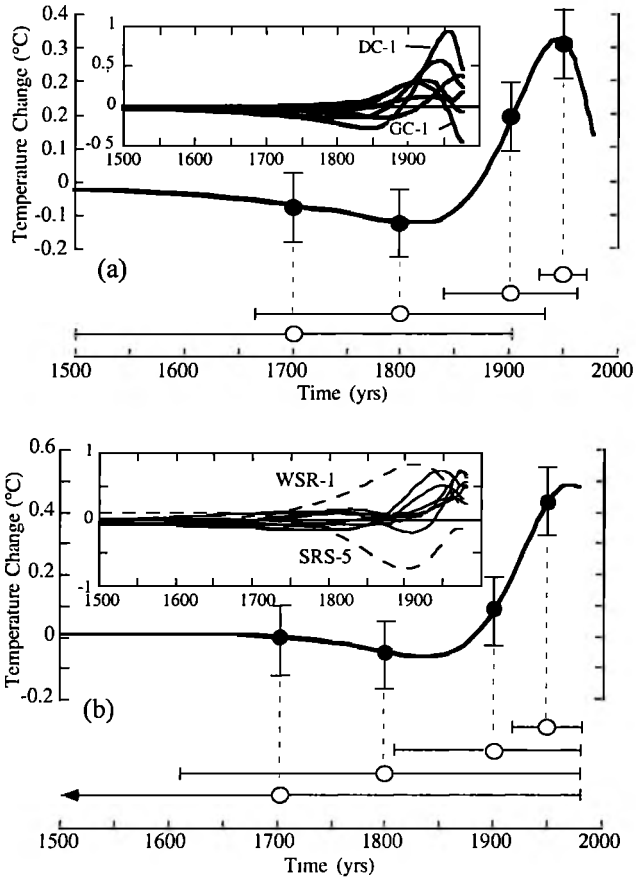

Figure 4. Ground surface temperature (GST) histories for Utah. (a) Average ground surface temperature history for western Utah using a priori parameters σ_{ko} = 1.0 W m^{-1}K^{-1} and σ_{do} = 50 mK; inset shows individual GST histories for the six sites. (b) Average surface ground temperature history for southeastern Utah using a priori parameters σ_{ko} = 2.0 W m^{-1}K^{-1} and σ_{do} = 50 mK without boreholes SRS-5 and WSR-1; inset shows individual GST histories. GST histories for boreholes SRS-5 and WSR-1 are shown as dashed curves. Horizontal lines below average GST histories show the spread as a function of time.

To emphasize the regional signal, we averaged the individual GST solutions together for both western and southeastern Utah. *Pollack et al.* [1996] demonstrated that averaging GST solutions is equivalent to inverting the borehole temperature-depth data simultaneously. *Shen et al.* [1995] point out that the FSI algorithm is only mildly nonlinear, and thus for loose inversions, such as ours, nonlinearities have only a small effect on the average. Figures 4a and 4b show the average GST signal for western and southeastern Utah, respectively. Because of the temporal smearing, GST histories do not represent an actual temperature-time history but a temporally smeared version of it. To emphasize the degree of temporal smearing, we have selected a few discrete points and have plotted the spread (represented by the horizontal bars). For example, to resolve an event centered around 1700, the climatic event would have to have a duration of about 400 to 600 years. Thus the widely discussed "Little Ice Age" [*Lamb*, 1977], having a cool period centered around 1700 and a duration of about 300 years, is below the temporal resolution of these GST solutions. Detection of such a climatic event in a borehole temperature log would depend on reducing both measurement and geologic noise.

In western Utah (Figure 4a), the smeared GST history shows a dip of about 0.1°C in the mid-1800s followed by a peak around 1940 of about 0.3°C, and another dip to 1978 when the boreholes were logged. The smeared GST for southeastern Utah (Figure 4b), calculated without boreholes SRS-5 and WSR-1, exhibits relatively constant average temperatures to 1750, a slight dip of about 0.1°C at 1840, followed by an increase of 0.5°C to 1980, when the boreholes were logged. This GST history is similar to western Utah, although more attenuated, because of the larger a priori values of σ_{ko} and hence a loss in resolution. These GST histories, of course, must be interpreted together with the accompanying time averaging information (Figure 4).

Another approach to detecting GST events involves combining temperature-depth data with meteorological temperature data or with proxy temperature data [*Lachenbruch et al.*, 1988; *Chapman et al.*, 1992; *Cuffey et al.*, 1995]. We demonstrate [*Harris and Chapman*, this issue] the advantages of combining temperature-depth data and meteorological temperature data.

6. Conclusions

Geothermal temperature-depth data from western and southeastern Utah have been examined for evidence of warming trends using the functional space inverse algorithm of *Shen and Beck* [1990, 1991]. Of the 15 Utah borehole sites investigated, 13 sites yield positive reduced temperature anomalies that indicate recent surface warming, while two sites indicate negative reduced temperature anomalies. The anomalies have magnitudes up to 0.5°C and extend to depths between 100 and 200 m. The smeared GST history for western Utah indicates a slight cooling of about 0.1°C centered in the mid-1800s followed by a peak in warming around 1940 of about 0.3°C, followed by a cooling trend to 1978 when the boreholes were logged. The smeared GST history for southeastern Utah is similar to western Utah and indicates an onset of warming starting approximately in 1850 with a magnitude of about 0.5°C. Two boreholes in southeastern Utah (SRS-5 and WSR-1) are rejected because of their dissimilarity to other GST histories within the same region.

Subsurface transient temperature perturbations in boreholes beyond the clear signal of 20th century warming or cooling are small. Smearing of the reconstructed surface temperature history is severe. This study illustrates the desirability of reducing measurement noise in temperature logging toward the 1 mK level and accounting for geologic and site noise at the 10 mK level. These are both attainable goals [*Clow*, 1992; *Chisholm and Chapman*, 1992, Appendix A; *Chapman and Harris*, 1993] and will allow for more precise estimates of 19th century and earlier surface temperature histories.

Acknowledgments. We thank Alan Beck, Paul Shen, and Vladimir Cermak for helpful reviews of this manuscript and Paul Shen for the use of his FSI algorithm. This work was supported by the National Science Foundation (EAR-9104292 and EAR-9205031), grant project 92037 of the Czech—U.S. Science and Technology Cooperation Program, and the University of Utah Graduate Fellowship program.

References

Backus, G, and F. Gilbert, The resolving power of gross earth data, *Geophys. J. R. Astron. Soc*, *16*, 169-205, 1968.

Backus, G, and F. Gilbert, Uniqueness in the inversion of inaccurate gross Earth data, *Philos. Trans. R. Soc. London, A266*, 123-192, 1970.

Beltrami, H., and J. C. Mareschal, Recent warming in eastern Canada inferred from geothermal measurements, *Geophys. Res. Lett.*, *18*, 605–608, 1991.

Beltrami, H., and J. C. Mareschal, Ground temperature histories for central and eastern Canada from geothermal measurements: Little Ice Age signature, *Geophys. Res. Lett.*, *19*, 689–692, 1992.

Birch, F., The effects of Pleistocene climatic variations upon geothermal gradients, *Am. J. Sci.*, *246*, 729–760, 1948.

Bodell, J. M., and D. S. Chapman, Heat flow in the north-central Colorado Plateau, *J. Geophys. Res.*, *87*, 2869–2884, 1982.

Chapman, D. S., Heat flow and heat production in Zambia, Ph.D. thesis, 94 pp., Univ. of Mich., Ann Arbor, 1976.

Chapman, D. S., and R. N. Harris, Repeat temperature measurements in borehole GC-1, northwestern Utah: Towards isolating a climate-change signal in borehole temperature profiles, *Geophys. Res. Lett.*, *20*, 1891-1894, 1993.

Chapman, D. S., M. D. Clement, and C. W. Mase, Thermal regime of the Escalante Desert, Utah, with an analysis of the Newcastle geothermal system, *J. Geophys. Res*, *86*, 11,735–11,746, 1981.

Chapman, D. S., T. J. Chisholm, and R. N. Harris, Combining borehole temperature and meteorologic data to constrain past climate change, *Global Plant. Change*, *6*, 269–281, 1992.

Chisholm, T. J., and D. S. Chapman, Climate change inferred from borehole temperatures: An example from western Utah, *J Geophys. Res.*, *97*, 14,155–14,176, 1992.

Clow, G. D., The extent of temporal smearing in surface-temperature histories derived from borehole temperature measurements, *Global Plant. Change*, *6*, 81–86, 1992.

Cuffey, K. M., G. D. Clow, R. B. Alley, M. Stuiver, E. D. Waddington, and R. W. Saltus, Large Arctic temperature change at the Wisconsin-Holocene glacial transition, *Science*, *270*, 455-458, 1995.

Deming, D., Evidence for climatic warming in north America from analysis of borehole temperatures, *Science*, *268*, 1576, 1995.

Deming, D., and R. A. Borel, Evidence for climatic warming in north central Oklahoma from analysis of borehole temperatures, *J Geophys. Res.*, *100*, 22,017-22,032, 1995.

Folland, C. K., T. R. Karl, and K. Y. Vinnikov, Observed climate variations and change, in Climate *Change: The IPCC Scientific Assessment*, edited by J. T. Houghton, C. J. Jenkins and J. J. Ephraums, pp. 195-238, Cambridge Univ. Press, New York, 1990.

Gosnold, W. D., P. E. Todhunter, and W. Schmidt, The borehole temperature record of climatic warming in the mid-continent of North America, *Global Plant. Change*, *15*, 33-45, 1997.

Hansen, J., and S. Lebedeff, Global trends of measured surface air temperature. *J. Geophys. Res*, *92*, 13,345-13,372, 1987.

Harris, R. N, and D. S. Chapman, Climate change on the Colorado Plateau of eastern Utah inferred from borehole temperatures, *J Geophys. Res*, *100*, 6367-6381, 1995.

Harris, R N., and D. S Chapman, Geothermics and climate change, 2, Joint analysis of borehole temperature and meteorological data, *J. Geophys. Res*, this issue.

Karl, T. R., and R. G Quayle, Climate change in fact and in theory: Are we collecting the facts?, *Clim. Change*, *13*, 6-17, 1988.

Karl, T. R., and C. N. Williams Jr., An approach to adjusting climatological time series for discontinuous inhomogeneities, *J Clim.*, 26, 1744-1763, 1987.

Karl, T. R., C. N. Williams Jr., P. J. Young, and W. M. Wendland, A model to estimate the time of observation bias associated with monthly mean maximum, minimum, and mean temperatures for the United States, *J. Clim.*, *25*, 145-160, 1986.

Lachenbruch, A. H., and B. V. Marshall, Changing climate: Geothermal evidence from permafrost in the Alaskan Arctic, *Science*, *234*, 689–696, 1986.

Lachenbruch, A. H., T. T. Cladouhos, and R. W. Saltus, Permafrost temperature and the changing climate, in *Permafrost*, v. 3, Fifth International Conference on Permafrost, edited by K. Senneset, pp. 9-17, Tapir Publishers, Trondheim, Norway, 1988.

Lamb, H. H., *Climate, Present, Past and Future*, 835 pp., Methuen, New York, 1977.

Lane, E. C., Geotherms of the Lake Superior Copper County, *J. Geol.*, *42*, 113-122, 1923.

Lewis, T. J., (Ed.), Climatic Change Inferred From Underground Temperatures, *Global Plant. Change*, *6*, 281 pp., 1992.

Pollack, H. N., P. Y. Shen, and S. Huang, Inference of ground surface temperature history from subsurface temperature data: Interpreting ensembles of borehole logs, *Pure Appl. Geophys.*, *147*, 537-550, 1996.

Sass, J. H., A. H. Lachenbruch, and R. J. Monroe, Thermal conductivity of rocks from measurements on fragments and its application to heat flow measurements, *J. Geophys. Res.*, *76*, 3391–3401, 1971.

Shen, P. Y., and A. E. Beck, Least squares inversion of borehole temperature measurements in functional space, *J. Geophys. Res.*, *96*, 19,965-19,979, 1991.

Shen, P. Y., and A. E. Beck, Paleoclimate change and heat flow density inferred from temperature data in the Superior Province of the Canadian Shield, *Global Plant. Change*, *6*, 143–165, 1992.

Shen, P. Y., H. N. Pollack, S. Huang, and K. Wang, Effects of subsurface heterogeneity on the inference of climate change from borehole temperature data: Model studies and field examples from Canada, *J. Geophys. Res.*, *100*, 6383-6396, 1995.

Shen, P Y., H. N. Pollack, and S. Huang, Inference of ground surface temperature history form borehole temperature data: A comparison of two inverse methods, *Global Plant. Change*, *14*, 49-57, 1996.

Tarantola, A., *Inverse Problem Theory*, 613 pp., Elsevier, New York, 1987.

Tarantola, A., and B. Valette, Generalized nonlinear inverse problems solved using the least squares criterion, *Rev. Geophys.*, *20*, 219–232, 1982a.

Tarantola, A., and B. Valette, Inverse problems = Quest for information, *J. Geophys.*, *50*, 159-170, 1982b.

Wang, K., and T. J. Lewis, Geothermal evidence from Canada for a cold period before recent climatic warming, *Science*, *256*, 1003–1005, 1992.

Wang, K., T. J. Lewis, D. S. Belton, and P. Y. Shen, Differences in recent ground surface warming in eastern and western Canada: Evidence from borehole temperatures, *Geophys. Res. Lett.*, *21*, 2689-2692, 1994.

Wigley, T. M. L., and T. P. Barnett, Detection of the greenhouse effect in the observations, in *Climate Change: The IPCC Scientific Assessment*, edited by J. T. Houghton, C. J Jenkins and J. J. Ephraums, pp. 239-255, Cambridge Univ. Press, New York, 1990.

D.S. Chapman, Department of Geology and Geophysics, University of Utah, Salt Lake City, UT 84112. (email: dchapman@mines.utah.edu)

R.N. Harris, Rosenstiel School of Marine and Atmospheric Science, University of Miami, 4600 Rickenbacker Causeway, Miami, FL 33149. (email: rharris@rsmas.miami.edu)

(Received June 26, 1997; revised October 26, 1997;
accepted November 10, 1997.)